ACS SENSORS

Article

Cite This: ACS Sens. 2018, 3, 1632−1638

pubs.acs.org/acssensors

Design of Protein-Based Biosensors for Selective Detection of Benzene Groups of Pollutants

Shamayeeta Ray,[†] Santosh Panjikar,[‡,§] and Ruchi Anand*[,†,∥]

[†]Department of Chemistry, Indian Institute of Technology Bombay, Mumbai 400076, Maharashtra India

[‡]Department of Biochemistry and Molecular Biology, Monash University, Victoria 3800, Australia

[§]Australian Synchrotron, Victoria 3168, Australia

[∥]Wadhwani Research Center for Bioengineering, IIT Bombay, Mumbai 400076, India

Supporting Information

ABSTRACT: Benzene and its derivatives form a class of priority pollutants whose exposure poses grave risk to human health. Since benzene lacks active functional groups, devising specific sensors for its direct detection from a milieu of aromatics has remained a daunting task. Here, we report three engineered protein-based biosensors that exclusively and specifically detect benzene and its derivatives up to a detection limit of 0.3 ppm. Further, the biosensor design has been engineered to create templates that possess the ability to specifically discriminate between alkyl substituted benzene derivatives; such as toluene, *m*-xylene, and mesitylene. Interference tests with simulated wastewater samples reveal that the engineered biosensors can selectively detect a specific benzene compound in water samples containing a milieu of high concentrations of commonly occurring pollutants. This work demonstrates the potential of structure guided protein engineering as a competent strategy toward design of selective biosensors for direct detection of benzene group of pollutants from real time environmental samples.

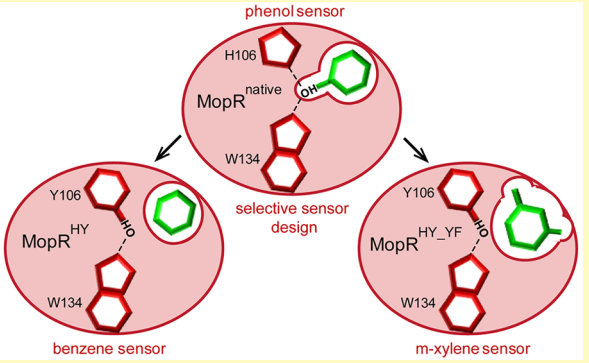

KEYWORDS: *MopR, benzene, m-xylene, mesitylene, protein engineering, selective biosensor*

Benzene and its derivatives, BTEX (benzene, toluene, ethylbenzene, xylene), are listed among the top 10 priority pollutants as per the United States Environmental Protection Agency (EPA) pollution database.[1] These xenobiotics contaminate the subsurface as well as groundwater due to leaching from underground gas storage tanks and landfills as well as from hazardous waste sites. At these sites, benzene based pollutants are present as a primary component of gasoline and petroleum products.[2,3] Exposure to benzene causes severe health hazards including central nervous system and immune system dysfunction and cancer.[4,5] In recent years, benzene spillage has caused havoc, such as in Lanzhou, China on April, 2014, where groundwater was contaminated, because of oil spillage, resulting in more than 2.4 million people being severely affected. Moreover, benzene pollution poses to be a serious threat as its hydrocarbon derivatives are highly resistant to degradation, and in absence of competent bacteria which can degrade them, these xenobiotics can accumulate in highly toxic concentrations in environmental wastewaters.[6]

From a sensing perspective, devising sensors for specific quantification of a specific BTEX is challenging. This is mostly because these hydrocarbons lack active functional groups, which makes direct detection methods difficult to implement. Currently, the most prevalent benzene sensors for air pollution monitoring are metal oxide based gas sensors.[7,8] A few cavitands based sensors that exploit CH−π interaction to select between BTEX have also been reported. However, in these systems, the sample has to be heated above 150 °C to attain any selectivity.[9] Fewer detection devices exist to monitor the levels of benzene compounds at ambient temperatures, such as in groundwater and wastewater samples. Gas chromatography−flame ionization detector (GC-FID) coupled with mass spectrometry constitutes the current established method of detection.[10−12] However, this method has limited portability and requires pretreatment and concentration of samples prior to any reasonable quantitative analysis.[13] Hence, there is a pressing need to develop simpler, easy to handle, specific and direct detection methods for in situ BTEX monitoring in wastewater samples.

A subclass of soil bacteria like *Pseudomonas* sp.[14,15] have adapted to survive in toxic aromatic pollutant environments by evolving proteins through natural selection that can specifically detect these xenobiotics and subsequently degrade them.[16] These regulatory sensor modules provide scaffolds for

Received: March 7, 2018
Accepted: August 7, 2018
Published: August 7, 2018

DOI: 10.1021/acssensors.8b00190
ACS Sens. 2018, 3, 1632−1638

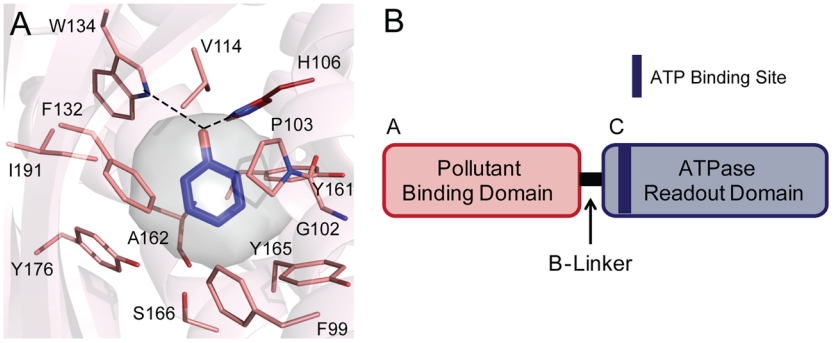

Figure 1. Design of in vitro biosensor. (A) Pollutant binding pocket of MopR where W134 and H106 anchor the phenolic OH group[28] Reprinted (in part) from ref 28. Copyright 2016 American Chemical Society. (B) Model design of in vitro biosensor based on MopR.

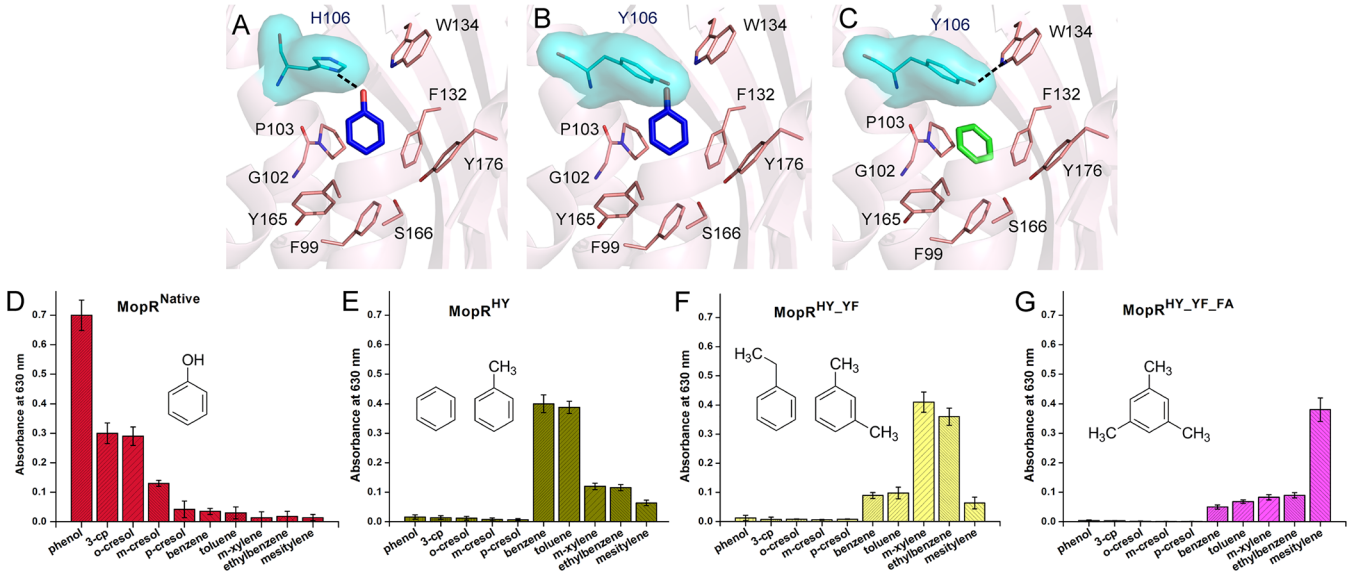

Figure 2. Selective in vitro biosensor designs for benzene and its derivatives. Panels (A−C) represent docked ligands for the following MopR mutants: (A) phenol with native MopR^{AB}, (B) phenol with MopR^{HY}, and (C) benzene with MopR^{HY}. The H106 residue in panel (A) and Y106 in panels (B) and (C) are in surface representation. Panels (D−G) represent in vitro biosensing ability of above sensor designs. The inducing concentration of all the aromatic compounds used in the assay is 10 μM.

development of specific biosensor design.[17−19] Nevertheless, extraction of these proteins with high yield and solubility in a suitable in vitro format has remained challenging.[20] For instance, the XylR protein, which is the natural benzene sensor, could only be extracted via urea denaturation and subsequent refolding techniques.[21] Hence, such proteins have been exploited till date in the frame of whole cell biosensors, allowing method of detection limits in the range of 0.1 μM within assays times of 2−3 h.[22−27] Very recently, we successfully obtained soluble protein for the phenol regulator, MopR from *Acinetobacter calcoaceticus* NCIB8250 and also solved the crystal structure of its pollutant sensing domain (MopR^{AB}).[28] The structure in complex with phenol and its derivatives serves as a representative of the XylR/DmpR subclass of pollutant sensing NtrC regulators and reveals the exact pollutant-binding pocket and the sensor residues (Figures 1A and S1). Members of this family possess a modular architecture consisting of an N-terminal signal sensing (A) domain that, upon pollutant binding, transmits the signal to the tandemly located AAA+ ATP dependent(C) domain[29,30] (Figure 1B). It is only upon activation that ATP hydrolysis occurs, which provides the readout for quantification of pollutant monitoring (Figure 1B). Substrate profiling of native MopR protein reveals that it is only capable of detecting smaller phenolics and is nonresponsive toward benzene and its derivatives (Figure 2D).[28,31] This is because the MopR pocket is specifically designed to anchor the phenolic OH group by hydrogen bonding with W134 and H106 (Figure 1A). Here, in this work, by utilizing the knowledge of the three-dimensional pocket architecture in conjunction with in silico and experimental approaches, we have tweaked the MopR sensor design and successfully created sensors that can exclusively sense BTEX and can even distinguish between alkyl substitutions on the benzene scaffold. Moreover, because these biosensors have been developed with purified proteins, this has reduced the response/assay time to 10−15 min making them more suitable candidates for pollutant monitoring in contaminated environmental wastewaters.

RESULTS AND DISCUSSION

The primary tool used for alteration of the substrate scope was structure guided protein engineering via targeted mutagenesis. The three main designed mutant constructs (listed in Experimental Section) were first screened in silico and only competent mutant protein−sensor pairs were further taken for experimentation. The benzene series of compounds lack the

DOI: 10.1021/acssensors.8b00190
ACS Sens. 2018, 3, 1632−1638

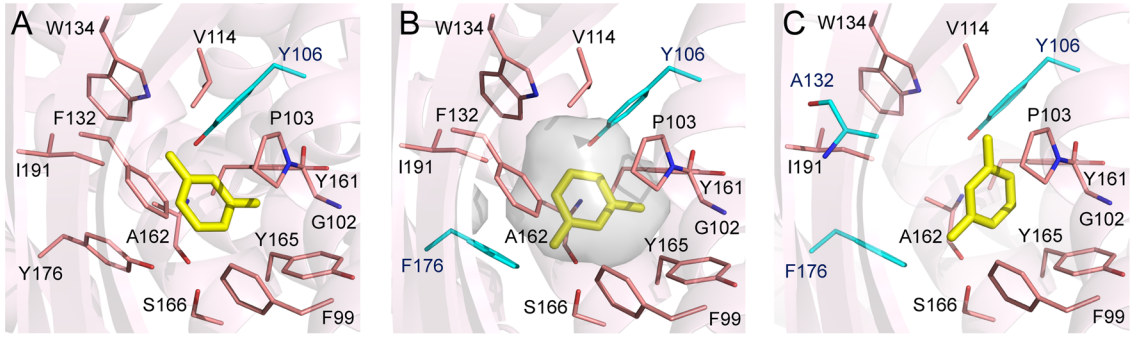

Figure 3. Structure guided selective sensing of *m*-xylene. Panels (A–C) represent docked *m*-xylene (in yellow) in the MopR mutant pockets: (A) MopR^{HY}, (B) MopR^{HY_YF}, and (C) MopR^{HY_YF_FA}. The MopR^{HY_YF} pocket exhibits the best geometry and energetics for *m*-xylene.

phenolic OH group. Therefore, in order to alter the substrate scope, the first mutation considered, required compensating for the interactions that anchor the primary phenolic ligand. The crystal structure reveals that both the imidazole group of H106 and the indole moiety of W134 partake in hydrogen bonding with the hydroxyl group of phenol (Figures 1A and 2A). Hence, the suggested design should have these interactions intrinsically satisfied by replacement of an appropriate amino acid that is able to retain the aromatic character of histidine as well as compensate for the interactions that were designed to stabilize the hydroxyl moiety. Analysis reveals that tyrosine residue, which possesses an aromatic hydroxyl group satisfies both these requirement. Thus, replacement of the histidine by a tyrosine residue, (H106Y mutant, MopR^{HY}) allows the tyrosine OH group to interact with the indole nitrogen atom of the W134 group, thereby leading to minimal change in pocket architecture (Figure 2B,C). Docking studies with an in silico MopR^{HY} mutation of the native pocket show that OH group of the tyrosine occupies the position of the phenolic OH and encounters a direct clash with the ligand, hence obliterating binding of all phenolic compounds (Figure 2B). It was observed that the overall pocket volume of the MopR^{HY} reduces to 143.6 Å^3 in the mutant in comparison to 158.3 Å^3 in the native structure and the pocket takes a shape such that the benzene can snugly be accommodated (Figures 2C and S3). Stacking interactions with the aromatic core of Y106 provide additional support, thereby yielding favorable binding energy scores (Table S1).

To validate the above hypothesis, supporting experiments were conducted and the mutant version of MopR^{HY} was cloned and purified (Experimental Section). The malachite green based in vitro colorimetic ATPase activity assay performed with a series of phenol and benzene derivatives (Figure S2) clearly showed that MopR^{HY} preferentially exhibits ATP hydrolysis in response to benzene and toluene and is completely nonresponsive to phenol and most of its derivatives (Figure 2E). For the moderately sized hydrocarbons like *m*-xylene, the sensor response was substantially reduced by almost 70% and only about 10% of the activity was retained for the trisubstituted bulkier ligands like mesitylene (Figure 2E). These results clearly indicate that the MopR^{HY} sensor activity has been primed to respond exclusively to smaller benzene derivatives leading to creation of an exclusive sensor for benzene and toluene. One of the intriguing questions that arose from the sensor activity data was how a single mutation in the sensor scaffold results in the biosensor discriminating between a monosubstituted toluene and disubstituted *m*-xylene (Figure 2E). To explain these observations, docking of the mutants with the mono-, di-, and trisubstituted series was undertaken (Figure S3). Results reveal that the shape of the pocket changes even by a single substitution and the pocket architecture of the MopR^{HY} is altered enough to select out alkyl substitutions. Comparison of the docked structures of toluene and *m*-xylene show that the presence of the additional methyl group in *m*-xylene results in a shift in the overall position of this compound, thereby creating a steric clash with residues like F132 that constitute the wall of the pocket (Figures 3A and S3). This yields a nonideal fit and lowers the binding energy of disubstituted benzene derivatives resulting in selective sensing (Figure S3). Bulkier hydrocarbons like mesitylene fare worse and are unable to even gain entry into the modified pocket (Figure S3D).

Our next goal was to design sensor models, which can selectively sense bigger alkyl substituted compounds. This is because many of the bulkier compounds like di- and trisubstituted benzenes constitute some of the commonly found environmental pollutants. To accommodate multiple alkyl group containing benzene derivatives, the primary strategy adopted was to increase the pocket volume of MopR^{HY} by retaining its hydrophobic character. Scanning through the pocket residues, it became apparent that the base of the pocket could be trimmed to create space. A series of in silico studies were performed and based on docking analysis, it was concluded that a minimal mutation of the tyrosine residue (Y176) to a phenylananine is sufficient to create space for *m*-xylene and other similar sized compounds. Docking with a series of benzene derivatives revealed that the MopR^{HY_YF} pocket fits best the moderately sized hydrocarbons like *m*-xylene and ethylbenzene (Table S1; Figures 3B and S4A). The MopR^{HY_YF} pocket allows the *m*-xylene ligand to orient such that both its methyl groups are accommodated in the space created at the base of the pocket (Figure 3B). Both smaller (benzene) and bulkier (mesitylene) derivatives exhibited reduced binding energies (Table S1, Figure S4). Due to the additional mutation, the increase in the pocket volume (150.3 Å^3) results in the benzene moiety no longer to be snuggly fitting in the MopR^{HY_YF} pocket (Figure S4B). On the other hand, for the bulkier benzene derivative, mesitylene, although the ligand could enter the pocket, but steric hindrance by the pocket wall residue such as F132, resulted in a scenario that was energetically unfavorable (Figure S4D). In silico studies further indicated that, among disubstituted aromatic derivatives, *m*-xylene is the most preferred isomer followed by *o*-xylene (Figure S5A,B). However, analysis reveals that the mutated pocket is shaped such that *p*-xylene is unable to fit in a

DOI: 10.1021/acssensors.8b00190
ACS Sens. 2018, 3, 1632–1638

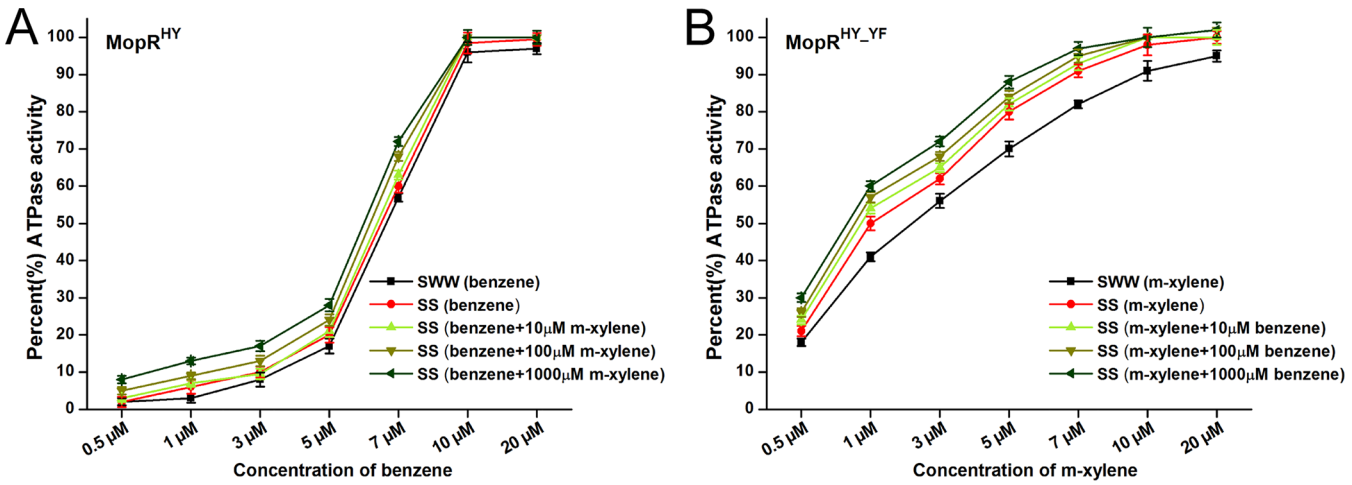

Figure 4. Interference tests on to gauge selectivity and sensitivity of biosensor designs. (A) Interference studies on the MopR^{HY} sensor where sensing of benzene (0.5−20 μM) in a simulated wastewater (SWW) sample (having 1 mM each of various noninducing pollutants, black curve) has been compared to standard solutions (SS) of benzene (red curve). Different green curves further represent interference tests in the presence of 10 μM (light green), 100 μM (olive green), and 1000 μM (bottle green) of a structurally homologous compound, *m*-xylene, mixed with benzene (0.5−20 μM) in the SS. (B) Interference studies on the MopR^{HY_YF} sensor where sensing of *m*-xylene (0.5−20 μM) in a simulated wastewater (SWW) sample (having 1 mM each of various noninducing pollutants, black curve) has been compared to standard solutions (SS) of *m*-xylene (red curve). Different green curves further represent interference tests in the presence of 10 μM (light green), 100 μM (olive green), and 1000 μM (bottle green) of a structurally homologous compound, benzene, mixed with *m*-xylene (0.5−20 μM) in the SS. Detailed compositions of the solutions that were tested have been provided in Experimental Section.

orientation conducive for signal transduction (Figure S5C) (detailed in the Supporting Information).

Experimental creation of the MopR^{HY_YF} double mutant, followed by purification confirms the in silico findings. In vitro ATPase assay with purified MopR^{HY_YF} confirmed that the hydrolysis activity is maximum in response to *m*-xylene and ethylbenzene sized derivatives (Figure 2F). Both for the smaller benzene as well as bulkier hydrocarbons, the ATPase activity is reduced by 70−80% (Figure 2F). Similarly, among the xylene isomers, *m*-xylene shows maximum activity followed by o-xylene which exhibits 80% activity, whereas the sensor exhibits poor sensitivity for *p*-xylene (Figure S5D). Surprisingly, the sensor also has dramatically reduced binding for toluene but good sensitivity for ethylbenzene. Analysis of the docked structure with toluene shows that pocket mutation changes the shape such that its methyl group comes in close proximity with the OH of Y106 (Figure S4C). However, the ethyl group of ethylbenzene owing to its kink, tilts the ligand which adopts a conformation such that the ethyl group snugly fits in the space between Y106 and W134 (Figure S4A). These results reiterate the fact that subtle changes in pocket architecture can yield in high selectivity among the BTEX class of compounds. Hence, MopR $^{HY\_YF}$ sensor design is inductive in stabilization of moderate sized benzenes like *m*-xylene, providing a framework for selective sensor design for medium sized benzene compounds.

An appropriate sensor framework for the bulkier hydrocarbons like mesitylene still remained a question. Hence, search for an apt mutation in the MopR^{HY_YF} pocket, which leads to a volume increment as well as retains the stability of the hydrophobic core was undertaken using previously described tools. A substitution of the phenylalanine residue by alanine (F132A) leads to the creation of the MopR^{HY_YF_FA} mutant, which exhibits an appropriate increase in pocket volume (201.8 Å^3) and is suitable to accommodate mesitylene (Figure S6A). Derivatives like benzene and *m*-xylene were no longer energetically favored, as the pocket volume was too large to lock these smaller ligands in unique orientations (Table S1, Figure 3C, S6). Creation of this triple mutation was experimentally undertaken and the in vitro ATPase assay with MopR^{HY_YF_FA} showed that maximum ATPase activity was observed in the presence of the bulky compound mesitylene (Figure 2G). Further, the triple mutant exhibited highly reduced ATP hydrolysis in response to the smaller benzene derivatives and was completely nonresponsive toward any of the phenol derivatives (Figure 2G). Based on these observations, it was inferred that MopR^{HY_YF_FA} serves as a model sensor design for selective sensing of bulkier toxic aromatic hydrocarbons. To further ascertain that all the designed sensor constructs were stable and changes in activity were not due to structural instability introduced by the mutations, confirmatory circular dichrosim studies were performed on all the mutants (Figure S7). No change or loss in secondary structure was observed for the experimentally tested mutants. Hence, it was concluded that all the observed alterations in activity for the MopR variants was a direct effect of the functional change and not attributed to any structural loss.

With the repertoire of these newly generated selective benzene based sensors, the next task was to test the viability and efficiency of these sensor designs in a realistic setting that is crowded by several pollutants of varied chemical profile. To test the sensor performance under harsh conditions, simulated wastewater (SWW) was generated by adding diverse range of chemicals at high concentrations (1 mM) like salts, metals, organics that are commonly found as pollutants in environmental wastewaters which are otherwise noninducers of MopR sensor activity (composition detailed in Experimental Section). Interference analysis on the MopR^{HY} and MopR^{HY_YF} sensor model systems was performed by adding varying concentrations (0.5−20 μM) of their best inducers (*m*-xylene in the case of MopR^{HY_YF} and benzene in the case of MopR^{HY}) to the SWW (black curves in Figure 4) and comparing the activity data with standard solutions(SS) of the inducers in the same

DOI: 10.1021/acssensors.8b00190
ACS Sens. 2018, 3, 1632−1638

concentration range (red curves in Figure 4). The concentration range chosen for testing interference was selected such that it spans limits that are well below the permissible toxicity limit of the contaminants as per EPA and OSHA. The aim was to gauge both selectivity and sensitivity of the biosensors when the random pollutants coexist with the target inducers. The $MopR^{HY}$ sensor pocket is efficiently tuned to only accept benzene and its closely related aromatics (toluene), and therefore, the presence of ions, salts, and phenolics only affected the signal by ∼3−5% (Figure 4A). Overall, it was observed that, for $MopR^{HY}$, there is negligible interference from the noninducers (in SWW) across the sensing concentration range of benzene (0.5−20 μM). This is likely because the $MopR^{HY}$ sensor pocket is too small for nonspecific interactions with other compounds thus, restricting undesired activity. Therefore, addition of random pollutants does not significantly seem to affect sensor performance in case of $MopR^{HY}$. On the other hand, in the case of $MopR^{HY\_YF}$ sensor design, for the noninducing pollutants in SWW, 5−10% competitive negative interference toward *m*-xylene sensing was observed (Figure 4B). This could be attributed to increased pocket size that now allows more type of substrates to enter the pocket allowing them to coexist with *m*-xylene.

Since it is possible that, in certain type of pollution scenario, both *m*-xylene and benzene may coexist, the interference of the $MopR^{HY}$ and $MopR^{HY\_YF}$ sensor constructs in the presence of both these structurally similar compounds were also gauged (Figure 4). Previous analysis clearly indicates that the ATPase signal is always biased toward the designed inducer for a particular sensor system by 80% or more (Figure 2E-G). However, to quantitatively determine the effect, three different concentrations (10, 100, and 1000 μM) of a structurally similar interferent were added to the standard solutions (SS) of the inducers (detailed in the Experimental Section). In the case of $MopR^{HY}$, the interference from *m*-xylene and in $MopR^{HY\_YF}$, the effects from benzene were tested (green curves in Figure 4A). For the $MopR^{HY}$ benzene sensor, the presence of *m*-xylene affected the signal minimally in the low to medium concentration ranges. Even at 10 times the *m*-xylene concentration, the signal was only enhanced by about 7−10% (Figure 4A). Thus, the $MopR^{HY}$ sensor is very robust for sensing smaller aromatics. In contrast, for benzene as a competitor of *m*-xylene in the pocket of $MopR^{HY\_YF}$, an additive effect was created which is about ∼10% at low concentrations of benzene (Figure 4B). In a mixture that has 10 times more benzene than *m*-xylene, the effect becomes more prominent (around ∼15−20%) (Figure 4B). However, the advantage of creating both the benzene specific $MopR^{HY}$ and *m*-xylene specific $MopR^{HY\_YF}$ sensors for monitoring this pollutant is that it allows for a direct comparison of their performance. The dual data enables the amount of each pollutant in the mixture to be evaluated. Especially, since the $MopR^{HY}$ benzene sensor exhibits low level of interference, the data from both sensors analyzed in conjunction allows estimation of individual amounts. The interference analysis highlights the importance of understanding the complex interactions and crosstalk between different pollutants and biosensors in a real-time scenario. Hence, for in situ monitoring, quantifying these effects aids in creation of efficient real-time sensors. Moreover, the MopR biosensor design is highly thermostable as well as requires low response time (minutes) to generate a substantial signal (Figure S8) and possesses both reasonable selectivity and sensitivity. All these factors coupled with exclusive shape-complementarity based biosensing design yield great potential for this system toward quantitative estimation of these benzene derivatives in real time contaminated environmental water bodies that harbor a milieu of different pollutants.

CONCLUSION

In conclusion, here we demonstrate that structure guided protein engineering is a powerful tool for creation of selective biosensor models. Architectures that were originally only tuned to sense phenol and its derivatives were modified by logic based tweaking to exclusively accept select BTEX compounds. Moreover, these direct detection protein-based sensors have the distinct advantage of possessing the ability to operate at ambient conditions. Furthermore, here, for the first time, we have been able to create sensors that can differentiate between methyl substituted benzene derivatives such as toluene, xylene, as well as mesitylene. These robust sensors are thermostable and do not exhibit substantial cross reactivity while retaining both selectivity and specificity in a milieu of environmental pollutants. The biosensing system serves as an important stepping stone to fuel development of commercial direct detection based low cost BTEX biosensors.

EXPERIMENTAL SECTION

Docking Studies. Based on the detailed analysis of the pollutant binding pocket using the phenol bound crystal structure of the signal sensing domain of MopR ($MopR^{AB}$)[28] (Figure S1), few site-specific mutations of the pocket residues were designed in silico. The first mutation designed was that of a tyrosine substitution of the key sensor residue H106 ($MopR^{HY}$). Further, to accommodate bulkier benzene derivatives with more than one substituent, two more mutations were designed sequentially in the $MopR^{HY}$ construct. They include (i) phenylalanine substitution of Y176 ($MopR^{HY\_YF}$) and (ii) alanine substitution of F132 ($MopR^{HY\_YF\_FA}$). Docking experiments using AutoDock version 4.2[32] of all these mutants were performed with phenol and a set of benzene derivatives (benzene, toluene, *m*-xylene, ethylbenzene, and mesitylene) (Figure S2). This was performed to predict alterations in specificity of MopR. A monomeric subunit of the X-ray structure of the $MopR^{AB}$-effector complex[28] (PDB code: 5KBE) was used for docking so as to predict affinity of the $MopR^{AB}$ mutants toward different pollutants. The template PDB used for the docking experiments was manually modified each time based on the mutants used. The final $MopR^{AB}$ mutant PDBs used for docking had the previously present ligand coordinates deleted from them. All docking runs were conducted by using a genetic algorithm (GA) in AutoDock version 4.2[32] against the target aromatic effectors. Each ligand for a particular mutant version of $MopR^{AB}$ was scored according to a free energy cost function (ΔG*) that accounts for van der Waals, hydrogen bonding, electrostatic, solvation, and torsional free energy terms. The grid box for docking was selected in the binding pocket region, and rigid docking was performed with 250 runs for each ligand−$MopR^{AB}$ mutant combinations. On the basis of the estimated free energy of binding (ΔG*) calculated in docking, the top-ranked ligand orientations were selected (listed in Table S1).

DNA Manipulations, Overexpression, and Purification of the Recombinant Proteins. To validate the docking results, the same set of in silico mutations of MopR ($MopR^{HY}$, $MopR^{HY\_YF}$, and $MopR^{HY\_YF\_FA}$) were experimentally incorporated into the native construct of MopR ($MopR^{ABC}$) from *Acinetobacter calcoaceticus* NCIB8250, that was previously cloned into modified pET vector.[33] All the point mutations were performed employing standard site-directed mutagenesis protocol using the "site-directed mutagenesis kit" from Kapa biosystems. The different mutant protein constructs were subsequently transformed into *Escherichia coli* BL21(DE3)plysS cells and grown at 37 °C until OD_{600} reached 0.6−0.8 and then induced with 0.7 mM IPTG (isopropyl-β-D-thiogalactopyranoside)

DOI: 10.1021/acssensors.8b00190
ACS Sens. 2018, 3, 1632−1638

and 5 mM $MgCl_2$ at 16 °C. All these mutants were expressed as C-terminal His tag fusion proteins and were purified using Ni-NTA resin employing standard His-tagged affinity purification protocol as described previously.[33] The eluted fractions were further concentrated and desalted with buffer containing 25 mM TRIS buffer, pH 7.5; 100 mM NaCl using an Econo- Pac 10DG (Bio-Rad, Hercules, CA) column. All the desalted fractions were pooled together and concentrated up to 6−8 mg/mL and were flash-frozen in liquid N_2, and stored at −80 °C until they were used.

Preparation of the Chemical Compounds. Saturated solutions (100 mM) of the volatile benzene derivatives were prepared in DMSO by shaking for few hours in a 37 °C incubator. Appropriate volumes of the saturated solutions were transferred to protein desalting buffer to achieve the desired liquid-phase concentrations (0.5−1000 μM) for each of the benzene compounds based on their mass balance and gas−liquid equilibrium as predicted by Henry's law coefficients at 37 °C[34] to make 1 mL working stocks in 1.5 mL eppendorfs. The working stock concentrations of the phenol derivatives, being nonvolatile, were diluted in protein buffer at appropriate concentrations from 100 mM stock solutions in water. All the saturated and working stock concentrations were reconfirmed by measuring their UV absorbance at λ_{max} and calculating their concentrations based on the extinction coefficient for each compound at their previously reported λ_{max} values.

In Vitro ATPase Assay. To perform the in vitro biosensing ATPase assay, 2 μM of protein sample (native and mutated $MopR^{ABC}$) was first incubated with 10 μM of each aromatic compound to be tested which, included the different phenol and benzene derivatives listed in Figure S2. The concentrations of all the compounds used in the assay correspond to ∼1−2 ppm which lie within the approximate environmental risk limits for these pollutants as per the Occupational Safety and Health Administration (OSHA). The ATPase assay was performed based on protocol reported previously.[33] All the absorbance values for the different $MopR^{ABC}$ constructs directly represent their absolute ATPase activity. Each of the experiments was performed in triplicate, and the error estimate has been represented as error bars within the figures.

Interference Assay with Simulated Wastewater (SWW) Sample. For performing the interference assay, the following types of solutions were first prepared: (a) standard solutions (SS) of inducers *m*-xylene (for the $MopR^{HY-YF}$ sensor) and benzene (for the $MopR^{HY}$ sensor) at a concentration range of (0.5−20 μM); (b) simulated wastewater (SWW) sample (mimicking a real time contaminated environmental sample) having the same concentration range of the inducer pollutants along with a mixture of different commonly found environmental pollutants (at 1 mM concentration of each interferent) including phenol, 3-chlorophenol, *o*-cresol (as representative phenol derivatives as part of volatile organic contaminants), NH_4^+ (as a representative cationic contaminant), Cl^- (as a representative anionic contaminant), and Co^{2+} (as a representative metal contaminant); (c) standard solutions (SS) of the inducer pollutants mixed with fixed concentrations (10, 100, and1000 μM) of structurally similar compounds; benzene (for the $MopR^{HY-YF}$ sensor) and *m*-xylene (for the $MopR^{HY}$ sensor). A concentration of 2 μM protein of the $MopR^{HY\_YF}$ mutant (which can preferentially sense *m*-xylene) and the $MopR^{HY}$ mutant (which can preferentially sense benzene) was first induced with their corresponding solutions of all three types and then tested for interference from other pollutants using the in vitro ATPase assay protocol as described above. The resultant ATPase activities in all the solutions were compared for analysis purposes. All the absorbance values have been represented as percent (%) ATPase activity. Each of the experiments was performed in triplicate, and the error estimate has been represented as error bars within the figure.

Circular Dichroism (CD) Studies. The native and mutant MopR proteins were tested (at 0.2 mg/mL each) for structural stability using CD studies. All the protein samples were prepared in phosphate buffer (25 mM sodium phosphate (pH-7.5), 80 mM NaCl). Scans were performed at 20 °C using 0.1 cm path length quartz cuvettes with 8 s differential integration time at a scan rate of 50 nm/s. For thermal stability analysis, the $MopR^{ABC}$ protein at 0.5 mg/mL was tested using a CD based thermal denaturation experiment. Scans were performed at a temperature range of 20−95 °C using 0.1 cm path length quartz cuvettes with 16 s differential integration time at a scan rate of 100 nm/s with 3 min delay time per temperature change.

■ ASSOCIATED CONTENT

Supporting Information

The Supporting Information is available free of charge on the ACS Publications website at DOI: 10.1021/acssensors.8b00190.

Crystal structure of the pollutant sensing domain of MopR; structures of aromatic compounds; selective sensing by $MopR^{HY}$ and $MopR^{HY\_YF}$; sensing response of $MopR^{HY\_YF}$ toward different isomers of xylene; selective sensing by $MopR^{HY\_YF\_FA}$; comparative CD between native and mutated MopR proteins; stability and response time of MopR biosensor; docking of $MopR^{AB}$ mutants with different aromatic pollutants (PDF)

■ AUTHOR INFORMATION

Corresponding Author

*E-mail: ruchi@chem.iitb.ac.in.

ORCID

Santosh Panjikar: 0000-0001-7429-3879

Ruchi Anand: 0000-0002-2045-3758

Author Contributions

S.R., R.A., and S.P. designed research; S.R. performed research; R.A. contributed new reagents/analytic tools; S.R., S.P., and R.A. analyzed data; and S.R. and R.A. wrote the paper.

Notes

The authors declare no competing financial interest.

■ ACKNOWLEDGMENTS

This work was funded by DST, Government of India (Grant Numbers EMR/2015/002121 and DST/TM/WTI/2K16/252).

■ REFERENCES

(1) Keith, L.; Telliard, W. ES&T Special Report: Priority pollutants: I-a perspective view. *Environ. Sci. Technol.* **1979**, *13* (4), 416−423.

(2) Weisel, C. P. Benzene exposure: An overview of monitoring methods and their findings. *Chem.-Biol. Interact.* **2010**, *184* (0), 58−66.

(3) Verma, D.; Tombe, K. Benzene in Gasoline and Crude Oil: Occupational and Environmental Implications. *AIHA J.* **2002**, *63*, 225−230.

(4) Falzone, L.; Marconi, A.; Loreto, C.; Franco, S.; Spandidos, D. A.; Libra, M. Occupational exposure to carcinogens: Benzene, pesticides and fibers. *Mol. Med. Rep.* **2016**, *14* (5), 4467−4474.

(5) Bahadar, H.; Mostafalou, S.; Abdollahi, M. Current understandings and perspectives on non-cancer health effects of benzene: A global concern. *Toxicol. Appl. Pharmacol.* **2014**, *276* (2), 83−94.

(6) Fuchs, G.; Boll, M.; Heider, J. Microbial degradation of aromatic compounds — from one strategy to four. *Nat. Rev. Microbiol.* **2011**, *9* (11), 803−816.

(7) Vaishnav, V. S.; Patel, S. G.; Panchal, J. N. Development of ITO thin film sensor for detection of benzene. *Sens. Actuators, B* **2015**, *206*, 381−388.

(8) Mabrook, M.; Hawkins, P. Benzene sensing using thin films of titanium dioxide operating at room temperature. *Sensors* **2002**, *2* (9), 374−382.

DOI: 10.1021/acssensors.8b00190
ACS Sens. 2018, 3, 1632−1638

(9) Trzcinski, J. W.; Pinalli, R.; Riboni, N.; Pedrini, A.; Bianchi, F.; Zampolli, S.; Elmi, I.; Massera, C.; Ugozzoli, F.; Dalcanale, E. Search of the Ultimate Benzene Sensor: The EtQxBox Solution. *ACS Sens.* **2017**, *2* (4), 590−598.
(10) Almeida, C. M. M.; Boas, L. V. Analysis of BTEX and other substituted benzenes in water using headspace SPME-GC-FID: method validation. *J. Environ. Monit.* **2004**, *6* (1), 80−88.
(11) Zwank, L.; Schmidt, T. C.; Haderlein, S. B.; Berg, M. Simultaneous Determination of Fuel Oxygenates and BTEX Using Direct Aqueous Injection Gas Chromatography Mass Spectrometry (DAI-GC/MS). *Environ. Sci. Technol.* **2002**, *36* (9), 2054−2059.
(12) Grbić-Galić, D.; Vogel, T. M. Transformation of toluene and benzene by mixed methanogenic cultures. *Appl. Environ. Microbiol.* **1987**, *53* (2), 254−260.
(13) Schweigkofler, M.; Niessner, R. Determination of Siloxanes and VOC in Landfill Gas and Sewage Gas by Canister Sampling and GC-MS/AES Analysis. *Environ. Sci. Technol.* **1999**, *33* (20), 3680−3685.
(14) Timmis, K. N.; Pieper, D. H. Bacteria designed for bioremediation. *Trends Biotechnol.* **1999**, *17* (5), 201−204.
(15) Diaz, E.; Prieto, M. A. Bacterial promoters triggering biodegradation of aromatic pollutants. *Curr. Opin. Biotechnol.* **2000**, *11* (5), 467−75.
(16) Tropel, D.; van der Meer, J. R. Bacterial transcriptional regulators for degradation pathways of aromatic compounds. *Microbiol. Mol. Biol. Rev.* **2004**, *68* (3), 474−500.
(17) O'Neill, E.; Ng, L. C.; Sze, C. C.; Shingler, V. Aromatic ligand binding and intramolecular signalling of the phenol-responsive σ54-dependent regulator DmpR. *Mol. Microbiol.* **1998**, *28* (1), 131−141.
(18) Rappas, M.; Bose, D.; Zhang, X. Bacterial enhancer-binding proteins: unlocking sigma54-dependent gene transcription. *Curr. Opin. Struct. Biol.* **2007**, *17* (1), 110−6.
(19) Shingler, V.; Moore, T. Sensing of aromatic compounds by the DmpR transcriptional activator of phenol-catabolizing Pseudomonas sp. strain CF600. *J. Bacteriol.* **1994**, *176* (6), 1555−60.
(20) Wikstrom, P.; O'Neill, E.; Ng, L. C.; Shingler, V. The regulatory N-terminal region of the aromatic-responsive transcriptional activator DmpR constrains nucleotide-triggered multimerisation. *J. Mol. Biol.* **2001**, *314* (5), 971−84.
(21) Kim, M. N.; Park, H. H.; Lim, W. K.; Shin, H. J. Construction and comparison of Escherichia coli whole-cell biosensors capable of detecting aromatic compounds. *J. Microbiol. Methods* **2005**, *60* (2), 235−245.
(22) Kobatake, E.; Niimi, T.; Haruyama, T.; Ikariyama, Y.; Aizawa, M. Biosensing of benzene derivatives in the environment by luminescent Escherichia coli. *Biosens. Bioelectron.* **1995**, *10* (6), 601−605.
(23) Ikeno, S.; Ogino, C.; Ito, T.; Shimizu, N. Detection of benzene derivatives by recombinant E. coli with Ps promoter and GFP as a reporter protein. *Biochem. Eng. J.* **2003**, *15* (3), 193−197.
(24) Di Gennaro, P.; Bruzzese, N.; Anderlini, D.; Aiossa, M.; Papacchini, M.; Campanella, L.; Bestetti, G. Development of microbial engineered whole-cell systems for environmental benzene determination. *Ecotoxicol. Environ. Saf.* **2011**, *74* (3), 542−549.
(25) Stiner, L.; Halverson, L. J. Development and Characterization of a Green Fluorescent Protein-Based Bacterial Biosensor for Bioavailable Toluene and Related Compounds. *Appl. Environ. Microbiol.* **2002**, *68* (4), 1962−1971.
(26) Tecon, R.; Beggah, S.; Czechowska, K.; Sentchilo, V.; Chronopoulou, P.-M.; McGenity, T. J.; van der Meer, J. R. Development of a Multistrain Bacterial Bioreporter Platform for the Monitoring of Hydrocarbon Contaminants in Marine Environments. *Environ. Sci. Technol.* **2010**, *44* (3), 1049−1055.
(27) Shingleton, J. T.; Applegate, B. M.; Nagel, A. C.; Bienkowski, P. R.; Sayler, G. S. Induction of the tod Operon by Trichloroethylene in Pseudomonas putida TVA8. *Appl. Environ. Microbiol.* **1998**, *64* (12), 5049−5052.
(28) Ray, S.; Gunzburg, M. J.; Wilce, M.; Panjikar, S.; Anand, R. Structural Basis of Selective Aromatic Pollutant Sensing by the Effector Binding Domain of MopR, an NtrC Family Transcriptional Regulator. *ACS Chem. Biol.* **2016**, *11* (8), 2357−2365.
(29) Shingler, V. Signal sensing by σ54-dependent regulators: derepression as a control mechanism. *Mol. Microbiol.* **1996**, *19* (3), 409−416.
(30) Studholme, D. J.; Dixon, R. Domain architectures of sigma54-dependent transcriptional activators. *J. Bacteriol.* **2003**, *185* (6), 1757−67.
(31) Schirmer, F.; Ehrt, S.; Hillen, W. Expression, inducer spectrum, domain structure, and function of MopR, the regulator of phenol degradation in Acinetobacter calcoaceticus NCIB8250. *J. Bacteriol.* **1997**, *179* (4), 1329−1336.
(32) Morris, G. M.; Huey, R.; Lindstrom, W.; Sanner, M. F.; Belew, R. K.; Goodsell, D. S.; Olson, A. J. AutoDock4 and AutoDockTools4: Automated docking with selective receptor flexibility. *J. Comput. Chem.* **2009**, *30* (16), 2785−91.
(33) Ray, S.; Panjikar, S.; Anand, R. Structure Guided Design of Protein Biosensors for Phenolic Pollutants. *ACS Sens.* **2017**, *2* (3), 411−418.
(34) Chang, H. L.; Alvarez-Cohen, L. Transformation capacities of chlorinated organics by mixed cultures enriched on methane, propane, toluene, or phenol. *Biotechnol. Bioeng.* **1995**, *45* (5), 440−9.

DOI: 10.1021/acssensors.8b00190
ACS Sens. 2018, 3, 1632−1638